




Article

Emergence and Evolution of OXA-23-Producing ST46_{Pas}-ST462_{Oxf}-KL28-OCL1 Carbapenem-Resistant *Acinetobacter baumannii* Mediated by a Novel IS*Aba1*-Based Tn7534 Transposon

Haiyang Liu ^{1,2,3} , Xiaochen Liu ^{1,2,3} , Jintao He ^{1,2,3}, Linghong Zhang ^{1,2,3}, Feng Zhao ^{4,5}, Zhihui Zhou ^{1,2,3}, Xiaoting Hua ^{1,2,3,*}  and Yunsong Yu ^{1,2,3,*}

¹ Department of Infectious Diseases, Sir Run Run Shaw Hospital, Zhejiang University School of Medicine, Hangzhou 310016, China

² Key Laboratory of Microbial Technology and Bioinformatics of Zhejiang Province, Hangzhou 310016, China

³ Regional Medical Center for National Institute of Respiratory Diseases, Sir Run Run Shaw Hospital, Zhejiang University School of Medicine, Hangzhou 310016, China

⁴ Department of Clinical Laboratory, Sir Run Run Shaw Hospital, Zhejiang University School of Medicine, Hangzhou 310016, China

⁵ Key Laboratory of Precision Medicine in Diagnosis and Monitoring Research of Zhejiang Province, Hangzhou 310016, China

* Correspondence: xiaotinghua@zju.edu.cn (X.H.); yvys119@zju.edu.cn (Y.Y.)

Abstract: Carbapenem-resistant *Acinetobacter baumannii* (CRAB) isolates of global clone 1 (GC1) and global clone 2 (GC2) have been widely reported. Nevertheless, non-GC1 and non-GC2 CRAB strains have been studied less. In particular, no reports concerning sequence type 46 (ST46_{Pas}) CRAB strains have been described thus far. In this work, the genomic features and possible evolution mechanism of ST46_{Pas} OXA-23-producing CRAB isolates from clinical specimens are reported for the first time. Antimicrobial susceptibility testing of three ST46_{Pas} strains revealed identical resistance profiles (resistance to imipenem, meropenem, ciprofloxacin and the combination of cefoperazone/sulbactam at a 2:1 ratio). They were found to belong to ST46_{Pas} and ST462_{Oxf} with capsular polysaccharide 28 (KL28) and lipooligosaccharide 1 (OCL1), respectively. Whole-genome sequencing (WGS) revealed that all contained one copy of chromosomal *bla*_{OXA-23}, which was located in a novel IS*Aba1*-based Tn7534 composite transposon. In particular, another copy of the Tn7534 composite transposon was identified in an Hgz_103-type plasmid with 9 bp target site duplications (TSDs, ACAACATGC) in the *A. baumannii* ZHOU strain. As the strains originated from two neighboring intensive care units (ICUs), ST46_{Pas} OXA-23-producing CRAB strains may have evolved via transposition events or a *pdf* module. Based on the GenBank database, ST46_{Pas} strains were collected from various sources; however, most were collected in Hangzhou (China) from 2014 to 2021. Pan-genome analysis revealed 3276 core genes, 0 soft-core genes, 768 shell genes and 443 cloud genes shared among all ST46_{Pas} strains. In conclusion, the emergence of ST46_{Pas} CRAB strains might present a new threat to healthcare settings; therefore, effective surveillance is required to prevent further dissemination.

Keywords: CRAB; ST46_{Pas}; evolution; novel transposon; Tn7534; OXA-23



Citation: Liu, H.; Liu, X.; He, J.; Zhang, L.; Zhao, F.; Zhou, Z.; Hua, X.; Yu, Y. Emergence and Evolution of OXA-23-Producing ST46_{Pas}-ST462_{Oxf}-KL28-OCL1 Carbapenem-Resistant *Acinetobacter baumannii* Mediated by a Novel IS*Aba1*-Based Tn7534 Transposon. *Antibiotics* **2023**, *12*, 396. <https://doi.org/10.3390/antibiotics12020396>

Academic Editors: John E. Gustafson, Michael J. McConnell and Maria Lina Mezzatesta

Received: 30 November 2022

Revised: 23 January 2023

Accepted: 14 February 2023

Published: 16 February 2023



Copyright: © 2023 by the authors. Licensee MDPI, Basel, Switzerland. This article is an open access article distributed under the terms and conditions of the Creative Commons Attribution (CC BY) license (<https://creativecommons.org/licenses/by/4.0/>).

1. Introduction

Acinetobacter baumannii is an important pathogen that emerged only several decades ago, causing severe nosocomial infections due to its high-level resistance to various antimicrobial compounds, including carbapenems [1,2]. In 2019, the Centers for Disease Control and Prevention (CDC) recognized carbapenem-resistant *Acinetobacter* as one of the “Urgent Threats” and a top priority because of the limited options for treatment [3]. Carbapenem-resistant *A. baumannii* (CRAB) strains pose a tremendous global health issue, especially for hospitalized patients with immune dysfunction in intensive care units (ICUs) [4].

Research to date has established that the majority of CRAB isolates belong to global clone 1 (GC1) and global clone 2 (GC2), with GC2 being the most widespread clone worldwide [5]. Carbapenem resistance in *A. baumannii* strains is commonly mediated by OXA-23 oxacillinase [2,6]. Based on previous reports, the *bla*_{OXA-23} gene is most frequently located in IS*Aba1*-based transposons, namely Tn2006, Tn2008, Tn2009 and AbaR4-type resistance islands [2,7–9]. These transposons can embed into the chromosome or insert into plasmids via IS*Aba1*-mediated transposition events, during which the signature of 9 bp target site duplications (TSDs) is formed [7,10,11].

Thus far, clones that do not belong to GC1 or GC2 CRAB strains have neither been reported nor studied in any detail, with very few exceptions. Moreover, ST46_{Pas} *A. baumannii* has been a relatively rare clone until now. Only one investigation from 2019 in Germany reported a carbapenem-susceptible *A. baumannii* (CSAB) collected from an infected animal (a horse with conjunctivitis), which belongs to ST46_{Pas} *A. baumannii* [12]. Researchers only described the draft genome sequence of *A. baumannii* strain 161514. Based on the Oxford scheme, ST46_{Pas} *A. baumannii* strains could be assigned to ST462_{Oxf} and have a close genetic relationship with ST1333_{Oxf} strains. However, there have been no related studies concerning ST462_{Oxf} and ST1333_{Oxf} clones to date.

In the current study, we characterized genomic features and possible evolutionary events occurring in three ST46_{Pas} OXA-23-producing clinical CRAB isolates for the first time. The genetic environment of the *bla*_{OXA-23} gene was analyzed in detail using a combination of short-read Illumina and long-read MinION whole-genome sequencing (WGS). A novel IS*Aba1*-based transposon (Tn7534) or *pdif* module may play a key role in the resistance gene transfer of *bla*_{OXA-23} from the chromosome to a plasmid with an Hgz_103-type replicon. We also performed comparative genomics of all ST46_{Pas} strains available in public databases and conducted the pan-genome analysis of the clone for the first time.

2. Results

2.1. Antimicrobial Susceptibility Profiles, Resistance Determinants and Virulence Factors

We characterized the resistome of three strains, *A. baumannii* DETAB-C9, DETAB-P65 and ZHOU. Antimicrobial susceptibility testing (AST) revealed that DETAB-C9, DETAB-P65 and ZHOU isolates were all resistant to imipenem (8–32 mg/L), meropenem (16–64 mg/L), cefoperazone/sulbactam (2:1 ratio) (64 mg/L) and ciprofloxacin (>32 mg/L). The *A. baumannii* ZHOU strain possessed comparably high MICs to carbapenems. However, three strains were still susceptible to ceftazidime (4 mg/L), amikacin (8 mg/L), colistin (1 mg/L) and tigecycline (0.5–1 mg/L) and remained intermediate to cefoperazone/sulbactam at a 1:1 ratio (32 mg/L) (Table 1).

Table 1. Minimum inhibitory concentrations of antibiotics used in this study.

Isolates	Antibiotics ¹ Minimum Inhibitory Concentration (mg/L)								
	IMP	MEM	CAZ	SCF (1:1)	SCF (2:1)	AMI	CIP	COL	TGC
DETAB-C9	16	32	4	32	64	8	>32	1	1
DETAB-P65	8	16	4	32	64	8	>32	1	0.5
ZHOU	32	64	4	32	64	8	>32	1	0.5

¹ IMP = imipenem, MEM = meropenem, CAZ = ceftazidime, SCF (1:1) = cefoperazone/sulbactam (1:1 ratio), SCF (2:1) = cefoperazone/sulbactam (2:1 ratio), AMI = amikacin, CIP = ciprofloxacin, COL = colistin, TGC = tigecycline.

Four resistance genes were found in all three *A. baumannii* strains: *bla*_{OXA-23}, *bla*_{OXA-67}, *bla*_{ADC-26} and *ant*(3'')-IIa. In addition, DNA gyrase GyrA was discovered to have an amino acid mutation in position 81 (Ser81Leu), which may contribute to fluoroquinolones' resistance.

Several virulence factors were detected in the three *A. baumannii* strains, including *bau*ABCDEF, *bas*ABCDEFGH and *bar*AB encoding acinetobactin for iron uptake, poly-β-1,6-N-acetyl-d-glucosamine (PNAG) encoding the gene cluster *pga*ABCD, the outer-membrane-protein-related gene *ompA*, *pbpG* encoding PbpG for serum resistance, *csu*

operon encoding Csu pili and two-component regulatory system *bfmRS* involved in Csu expression. Additionally, the lipopolysaccharide (LPS)-related genes *lpxABC* and *lpxL* were also identified.

2.2. Transfer of Carbapenemase Resistance Determinants

Mating assays and chemical transformation were conducted to study the transferability of *bla*_{OXA-23}. However, despite several attempts, no transconjugants and transformants were obtained, possibly indicating that the determinants are not readily transferred.

2.3. Multilocus Sequence Typing (MLST), Capsular Polysaccharide (KL) and Lipooligosaccharide (OCL)

According to the Pasteur and Oxford MLST schemes, all three strains belong to ST46_{Pas} (*cpn60-5*, *fusA-12*, *gltA-11*, *pyrG-2*, *recA-14*, *rplB-9*, *rpoB-14*) and ST462_{Oxf} (*cpn60-16*, *gdhB-59*, *gltA-31*, *gpi-142*, *gyrB-33*, *recA-40*, *rpoD-7*).

To analyze the KL and OCL of strains, *Bautype* and *Kaptive* software were used. The strains DETAB-C9 and DETAB-P65 were found to contain KL28 and OCL1, matching the 100% coverage to the reference sequence with 97.41% and 98.75% identity, respectively. Likewise, the KL and OCL in *A. baumannii* ZHOU were identical to those in DETAB-C9 and DETAB-P65, with a nucleotide identity of 97.41% and 98.77%. Similarly, identical KL and OCL results were obtained using *Kaptive* and *Bautype*.

2.4. Chromosome Analysis of ST46_{Pas} Strains

A hybrid assembly of short reads and long reads was performed to generate the complete genome sequences of *A. baumannii* strains. All strains exhibited a circular chromosome with a size of approximately 4 Mb and a GC content of 39% (Table 2). The chromosome of the *A. baumannii* ZHOU isolate contained a copy of the novel IS*Aba1*-derived Tn7534 transposon. Corresponding to 28 bp site-specific recombinases XerC/XerD (C/D) and XerD/XerC (D/C) (also named *pdif*), 20 *pdif* sites were found in the chromosome of DETAB-C9 and DETAB-P65 strains. However, only 14 *pdif* sites were identified in the *A. baumannii* ZHOU chromosome, and *pdif* 2 and *pdif* 3 sites at each side of the *bla*_{OXA-23} segment (Table S1). In addition, no prophage regions were identified in the chromosome of the three clinical strains.

Table 2. Characteristics of genome components.

Isolates	Element	Replicon	Size (bp)	GC (%)	Antibiotic Resistance Genes
DETAB-C9	chromosome	ND	3,999,538	38.98%	<i>bla</i> _{OXA-23} , <i>bla</i> _{OXA-67} , <i>bla</i> _{ADC-26} , <i>ant</i> (3'')-IIa
	pDETAB-C9-1	Aci6	73,444	33.40%	Not detected
DETAB-P65	chromosome	ND	3,999,531	38.98%	<i>bla</i> _{OXA-23} , <i>bla</i> _{OXA-67} , <i>bla</i> _{ADC-26} , <i>ant</i> (3'')-IIa
	pDETAB7b	Aci6	73,444	33.40%	Not detected
ZHOU	chromosome	ND	4,057,466	39.02%	<i>bla</i> _{OXA-23} , <i>bla</i> _{OXA-67} , <i>bla</i> _{ADC-26} , <i>ant</i> (3'')-IIa
	pZHOU-1	Hgz_103	106,589	41.38%	<i>bla</i> _{OXA-23}
	pZHOU-2	Aci6	72,233	33.50%	Not detected

2.5. Genetic Analysis of Plasmids

We identified one plasmid each in DETAB-C9 and DETAB-P65, which we called pDETAB-C9-1 and pDETAB7b, respectively. Based on the analysis of replicons, they both belonged to the Aci6 type with a size of 73,444 bp (Table 2). A similar plasmid, a 72,233 bp Aci6-type plasmid (called pZHOU-2), was identified in the ZHOU isolate, with 33.50% GC content (Table 2). Interestingly, no resistance genes were found to be encoded in the Aci6-type plasmids (Figure 1A). In contrast to the other two strains, another Hgz_103-type plasmid was identified in the *A. baumannii* ZHOU isolate, which we named pZHOU-1. A second copy of the novel IS*Aba1*-based Tn7534 transposon was found in this plasmid, which exhibited the typical 9 bp target site duplications (TSD; ACAACATGC) (Figure 1B).

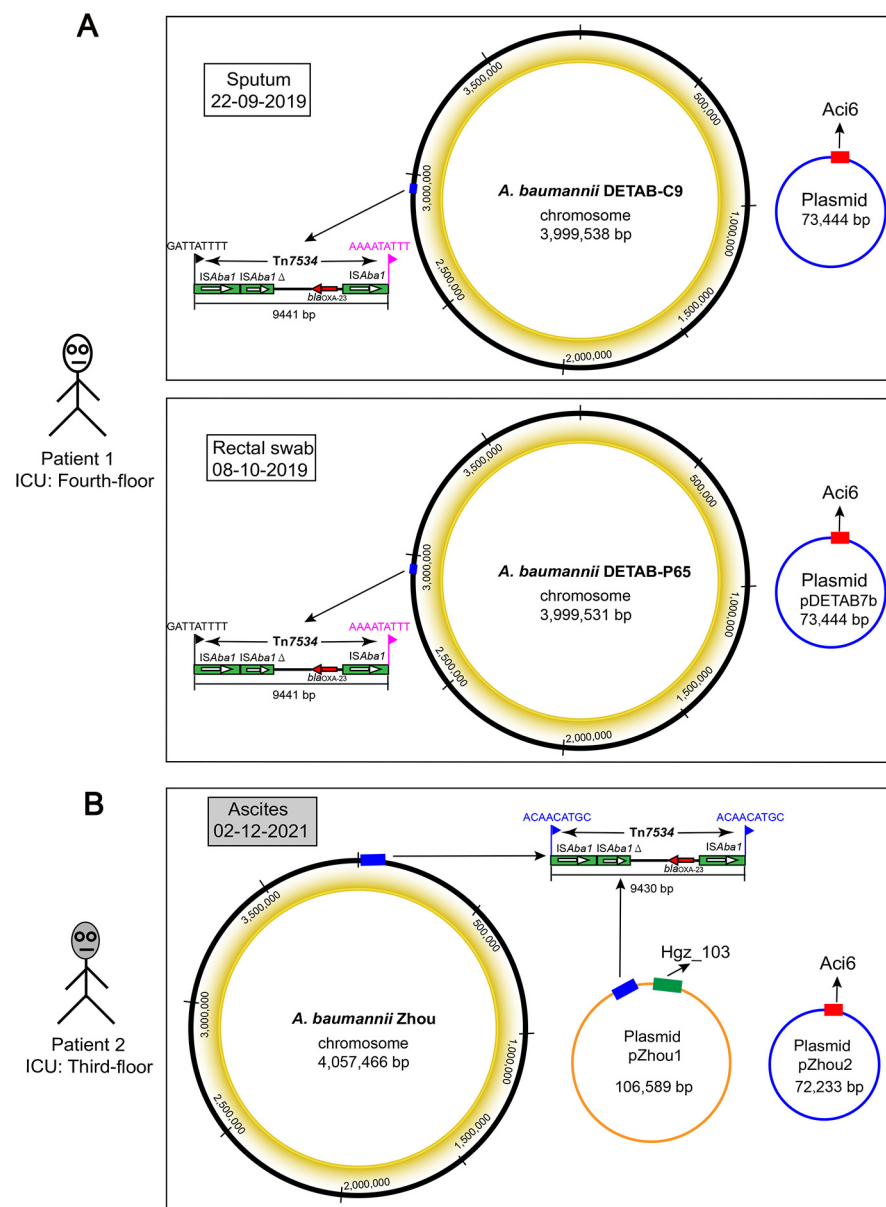


Figure 1. *A. baumannii* strains and genomic information. (A) *A. baumannii* DETAB-C9 and DETAB-P65 were collected from the sputum and rectal swab of patient 1 (upper white cartoon character) on the fourth floor of the ICU. Circular maps of the chromosome and plasmid are shown using black and blue circles, respectively. The position of novel transposon Tn7534 is indicated by the blue box, and its specific structure is drawn with 9 bp target site duplications (TSDs) indicated using different-colored flags based on the TSD sequence. (B) The *A. baumannii* ZHOU strain was collected from ascites of patient 2 (lower grey cartoon character) on the third floor of the ICU in the same hospital. Circular maps of the chromosome and plasmid are also shown. The Hgz_103-type plasmid is indicated by an orange circle. Two copies of Tn7534 transposon are indicated by a blue box with 9 bp identical TSDs (ACAACATGC) on either side.

2.6. Plasmid Comparison and the Evolution of ST46_{Pas} CRAB Mediated by a Novel Tn7534 Transposon

With 99.99% identity and 94% coverage, the plasmid pZHOU-1 was identical to the *A. baumannii* ZW85-1 plasmid ZW85p2 (GenBank accession CP006769), first isolated in 2013 in Beijing (Figure 2A,B). However, no *oriT* or mobile genetic elements (MGEs) were found in the pZHOU-1 plasmid.

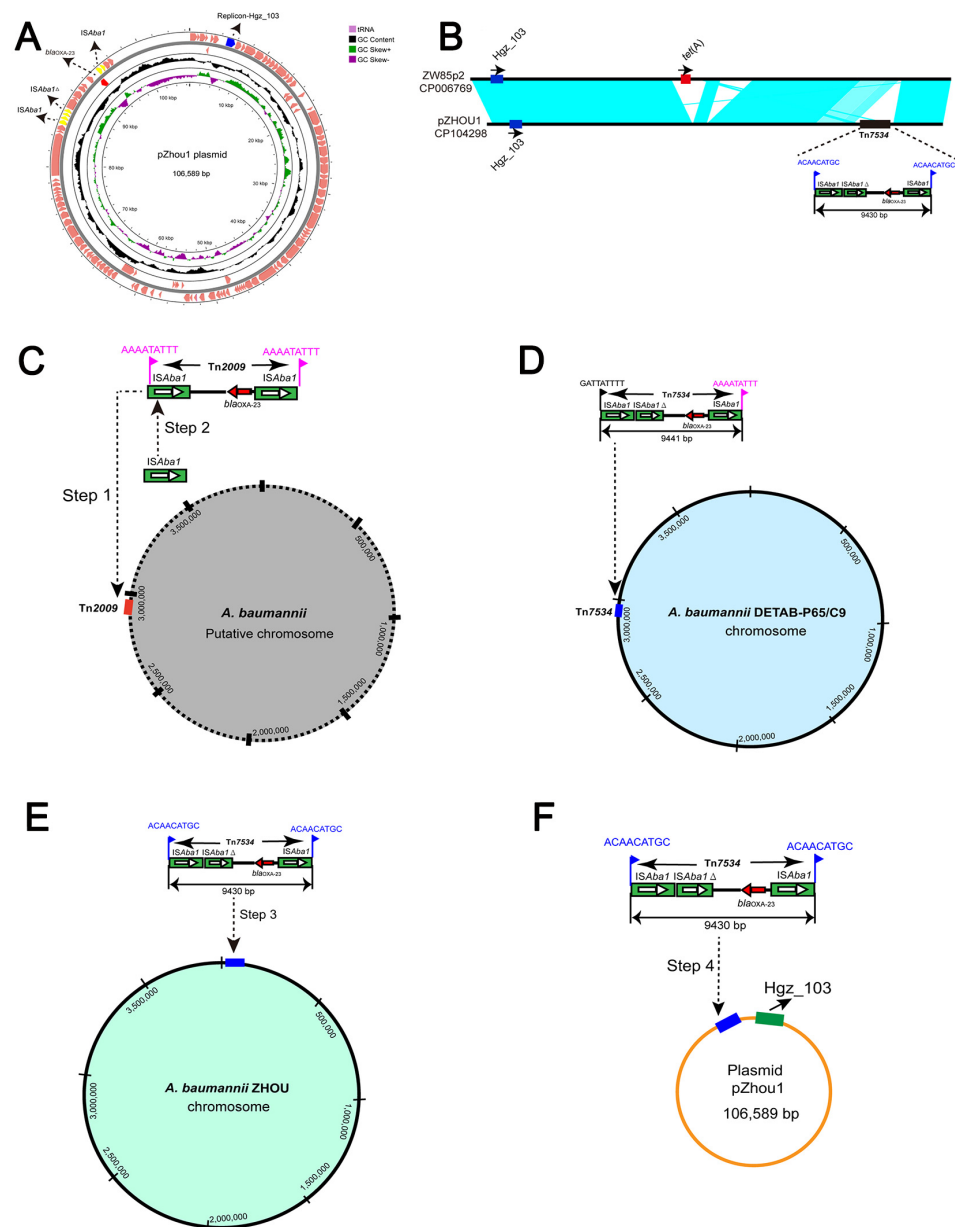


Figure 2. Circular map of Hgz-103-type plasmid pZhou1 and comparison with ZW85p2 and the proposed diagram for the evolution of ST46_{Pas} CRAB. **(A)** Circular map of Hgz-103-type pZhou1 plasmid. Arrows show the direction of ORFs. Red arrow indicates the *bla*_{OXA-23} gene. Blue arrow indicates the Hgz-103 replicon. Yellow arrows represent ISAbal1. **(B)** Linear maps and comparison with the ZW85p2 plasmid (accession number: CP006769). Blue arrows indicate the Hgz-103 replicons, with black arrows indicating the direction of ORFs. Red box indicates the resistance gene *tet*(A). The Tn7534 transposon is shown and labeled with a 9 bp TSD (ACAACATGC). Homologous segments (representing $\geq 99\%$ identity) are indicated by light blue shading. **(C)** The putative ST46_{Pas} chromosome circle map. Tn2009 transposon is indicated by a red box with a 9 bp TSD (AAAATATTT). The *bla*_{OXA-23} gene is shown by the red arrow. ISAbal1 is indicated by a green box with a white arrow. The complete Tn2009 composite transposon was integrated into the putative *A. baumannii* chromosome, followed by another copy of ISAbal1, which interrupted the original ISAbal1, contributing to generating ISAbal1 Δ to form transposon Tn7534 in *A. baumannii* DETAB-C9 or DETAB-P65, as shown in **(D)**. **(E,F)** The Tn7534 composite transposon was integrated into the *A. baumannii* ZHOU chromosome and pZhou1 plasmid. The 9 bp TSDs (ACAACATGC) are indicated by blue flags.

We then attempted to verify the evolutionary hypothesis about how the OXA-23-producing ST46_{Pas} CRAB originated. In detail, in step 1, a complete Tn2009 composite transposon harboring *bla*_{OXA-23} was inserted into the *A. baumannii* chromosome to form 9 bp TSDs (AAAATATTT) flanking both sides (Figure 2C). Following this event, another copy of *IS**Aba1* interrupted the original *IS**Aba1*, possibly contributing to the generation of *IS**Aba1*Δ and the formation of the novel transposon Tn7534 (Figure 2D). Eventually, the Tn7534 composite transposon was likely to integrate into the chromosome (Figure 2E). At one point, which cannot be conclusively determined from the sequence data (in parallel, before or after the genomic integration), the transposon was inserted into the pZHOU1 plasmid (Figure 2F), causing an 11 bp deletion that led to the formation of the signature 9 bp TSD (ACAACATGC).

2.7. Phylogenetic Analysis of All ST46_{Pas} *A. baumannii* Strains from NCBI Database

To further analyze the characteristics of ST46_{Pas} *A. baumannii* strains, a query using the NCBI GenBank database was performed. We found sequences of eight other ST46_{Pas} *A. baumannii* strains. Based on the MLST type of the Oxford scheme, all strains, apart from *A. baumannii* strain 161514, belonged to ST462_{Oxf}. According to the previously published data, *A. baumannii* strain 161514 belonged to ST462_{Oxf} as well; however, it exhibited a mutation in *gdhB* (Oxf_ghdB_59 A > T). We then reanalyzed sequences that showed the strain belonged to a new ST_{Oxf}, namely ST2098_{Oxf}. Isolates were collected in Germany or China from several sources, including rectal swabs, conjunctivitis, sputum, blood and ascites, between 2014 and 2021 (Figure 3A). The hosts were mainly human, but—as previously mentioned—one strain was isolated from a horse (*Equus ferus caballus*). All ST46_{Pas} *A. baumannii* strains, which were collected from patients in Hangzhou (China), contained the *bla*_{OXA-23} gene. In contrast, no *bla*_{OXA-23} gene was identified in *A. baumannii* strain 161514 isolated from the equine in Germany. Genetic relationship analysis showed a rather close genetic connection between the two strains, DETAB-C9 and DETAB-P65. Additionally, three other strains (AB_HZ_B30, AB_HZ_S30, AB_HZ_B28) collected from another hospital but the same city, Hangzhou, were closely related.

2.8. Pan-Genome and Single Nucleotide Polymorphisms (SNPs) Analysis

SNP analysis data illustrate the large diversity of ST46_{Pas} *A. baumannii* strains. The DETAB-C9 and DETAB-P65 strains were found to be closely related, with only a 16-SNP difference observed (Figure 3B). A total of 18 to 33 SNPs were found in the AB_HZ_B30, AB_HZ_S30 and AB_HZ_B28 strains. In terms of the number of SNPs, there were large differences in the *A. baumannii* strain 161514 isolated in Germany when compared to the other strains, which were first found in China.

The genomes of all available ST46_{Pas} *A. baumannii* strains were re-annotated. We then performed a gene presence/absence analysis. Bioinformatic data revealed 3276 core genes, 0 soft-core genes, 768 shell genes and 443 cloud genes (Figure S1A). The presence/absence of genes were visualized with the phylogenetic tree (Figure S1B).

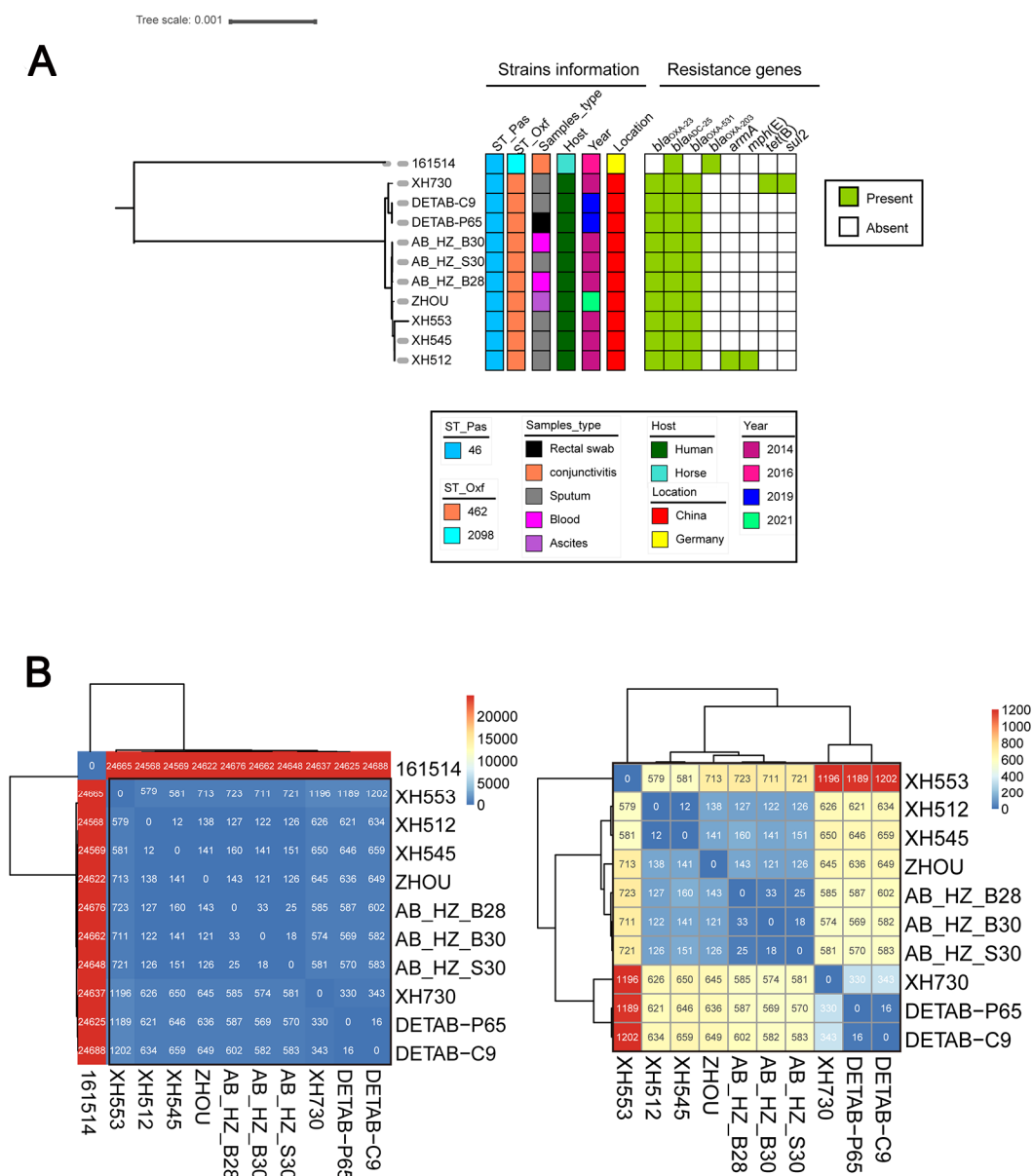


Figure 3. Phylogenetic analysis of 11 ST46_{PaS} *A. baumannii* strains and SNPs matrix values among ST46_{PaS} strains. **(A)** The tree was built with Snippy v4.4.5 and FastTree using RAxML under the GTRGAMMA model with DETAB-C9 as the reference strain and visualized with iTOL v5. Isolate name, Pasteur and Oxford MLST schemes, sample type, host, collection locations, isolation date and the heatmap of resistance genes are shown for each strain. The GenBank accession numbers of other ST46_{PaS} *A. baumannii* strains from the NCBI GenBank public database are as follows: 161514 (GenBank accession number: RPKD01000001), XH730 (GenBank accession number: LYHV01000001), AB_HZ_B30 (GenBank accession number: PRIR01000001), AB_HZ_S30 (GenBank accession number: PRFV01000001), AB_HZ_B28 (GenBank accession number: PRJO01000001), XH553 (GenBank accession number: LYKU01000001), XH545 (GenBank accession number: LYLC01000001), XH512 (GenBank accession number: LYL01000001). **(B)** SNP matrix values among ST46_{PaS} strains. SNP differences are indicated as numbers in the boxes. Strains in the black square are the same.

3. Discussion

Hospital-acquired infections caused by CRAB strains pose a growing clinical problem that has become a concern worldwide [13–15]. CRAB strains can persist in the hospital environment outside of patients, while at infection sites, they can form biofilms, further

complicating treatment. Especially in the ICU, accidental dissemination can lead to infections in immunocompromised patients admitted due to non-infection-related medical issues [16–18].

In this work, we describe the first complete genome sequences of ST46_{PaS} and ST462_{Ox}f strains, which were collected from ICU patients in China. In 2019, Wareth et al. described a single draft genome sequence of a CSAB isolate recovered from a horse with conjunctivitis in Germany [12]. To our knowledge, this study is the first comprehensive report of ST46_{PaS} CRAB strains that also explores possible evolutionary pathways, including the integration and dissemination of composite transposons.

The regions encoding genes for the biosynthesis of capsular polysaccharide (KL) and the lipooligosaccharide outer core (OCL) are potentially highly valuable markers for tracking closely related isolates and assisting epidemiological surveillance in the hospital setting [19]. A well-conducted study by Wyres et al. established that OCL1 (2086/3029, 68.87%) was the most common type, followed by OCL3 (272/3029, 8.98%) [19]. Consistent with this observation, we observed that our strains contained OCL1, to a high degree of confidence. Moreover, by analyzing the KL type of genome assemblies downloaded from the NCBI GenBank database, we found that the most common KL types were KL2 (713/2948, 24.2%), KL9 (343/2948, 11.6%) and KL22 (330/2948, 11.2%) [19]. Hence, *A. baumannii* DETAB-C9, DETAB-P65 and ZHOU strains all exhibited a relatively rare type, KL28.

Mobile genetic elements (MGEs), including insertion sequences (ISs), integrons (In) and transposons (Tn), play a crucial role in antimicrobial resistance gene (ARG) transfer among different kinds of pathogens or between the chromosome and plasmids in a strain [20,21]. Here, the IS26 transposase, a member of the IS6 family, has the remarkable capability to spread ARGs across many Gram-negative bacteria [22,23], especially *Klebsiella pneumoniae* [24] and *E. coli* [25]. However, in *A. baumannii*, IS*Aba1*-based composite transposons are associated with carbapenem resistance and their transfer [8]. Here, we delineated the possible evolutionary pathway of the genetic segment containing *bla*_{OXA-23}. The segment harboring *bla*_{OXA-23} likely emerged and transferred via translocation events of the novel IS*Aba1*-related Tn7534 transposon. Previous studies uncovered that site-specific recombinases XerC/XerD (C/D) and XerD/XerC (D/C) are able to mediate ARG transfer, including that of *tet*(39) [26], *bla*_{OXA-24} [27] and *bla*_{OXA-58} [1]. In our study, we identified two C/D and D/C *pdif* sites near the Tn7534 transposon containing the *bla*_{OXA-23} gene. The DNA segment encompassing the C/D and D/C *pdif* sites, including the Tn7534 transposon, possibly forms a *pdif* module. Based on this data, we inferred that another possible mechanism of the mobilization of the Tn7534 transposon containing the carbapenemase gene *bla*_{OXA-23} was the recombinase proteins XerC and XerD. A previous study revealed that prophage regions occasionally contain different resistance genes in *A. baumannii* strains, especially for *bla*_{NDM-1} and *bla*_{OXA-23}, demonstrating an important role of phages in the transfer of ARGs [28]. In contrast to this report, we were unable to identify prophage regions in our three clinical strains. Consequently, phage-mediated transduction of the *bla*_{OXA-23} carbapenem resistance gene is unlikely for the strains we investigated.

Of note is the finding that all ST46_{PaS} CRAB strains were isolated in Hangzhou (China), as far back as 2014. This illustrates that ST46_{PaS} CRAB strains have existed in China for at least 8 years. Fortunately, its spread to other locations in the world has not been reported thus far. Our comprehensive pan-genome analysis, which highlighted the similarity of the strains based on the shared 3276 core genes, also revealed the diversity of the isolates, which we assessed on the basis of the differences in SNPs.

While our study aimed to characterize ST46_{PaS} CRAB strains, there were also limitations to our work. One is that we previously found the *A. baumannii* ZHOU strain to possess a hypermucoviscous phenotype, for which the virulence level could be further assessed [10]. Likely more important is the fact that we failed to establish the transferability of the Hgz_103-type plasmid harboring *bla*_{OXA-23} within the Tn7534 transposon via conjugation or chemical transformation. One possible reason for this is that a T4SS-related transfer (*tra*) system, *oriT* region and relaxase were not identified in this plasmid, explaining the

failure of our conjugation experiments. With regard to the transformation experiments, the uptake of DNA fragments via natural transformation with fragments larger than 50 kb is a challenge for bacteria [29]. Moreover, co-mobilization with another conjugative plasmid or the transfer via outer membrane vesicles could be explored. The lack of rapid and frequent transfer via any of the above mechanisms might explain the locally contained presence of the strains.

4. Materials and Methods

4.1. Patient Information, Bacterial Isolation and Identification

DETAB-C9 was isolated from the sputum of an 85-year-old male patient in the fourth-floor ICU of our hospital in Hangzhou, China, on 22 September 2019. This patient underwent screening of an oral swab and rectal swab every week. DETAB-P65 was collected from the rectal swab on 8 October 2019 from the same patient. In brief, the rectal swab was placed in 2 mL of tryptic soy broth (TSB) with 0.1% sodium thiosulfate and then incubated at 37 °C for one day. Then, 20 µL of overnight culture was plated onto *Acinetobacter* sp. CHROMagar plates (CHROMagar, Paris, France), which were supplemented with 2 mg/L meropenem. After 24 h of static culture at 37 °C, a single colony was chosen according to its color (red) and morphology, then streaked onto a Mueller–Hinton (MH) agar plate (Oxoid, Hampshire, UK), incubated overnight at 37 °C. A single colony was selected. Isolate identification was performed via matrix-assisted laser desorption ionization–time of flight mass spectrometry (MALDI-TOF MS; bioMérieux, Marcy-l'Étoile, France) and further confirmed via 16S rRNA gene-based PCR and sequencing.

A. baumannii strain ZHOU was collected from ascites in the clinical laboratory during the routine diagnostic of another 63-year-old male patient in the third-floor ICU of the same hospital on 2 December 2021.

4.2. Antimicrobial Agent Susceptibility Testing

Antimicrobial susceptibility against imipenem, meropenem, ceftazidime, cefoperazone/sulbactam (1:1 ratio), cefoperazone/sulbactam (2:1 ratio), amikacin, ciprofloxacin, colistin and tigecycline was determined using the broth microdilution method according to Clinical Laboratory Standards Institute (CLSI) 2021 standards. In particular, susceptibilities of cefoperazone/sulbactam at 1:1 and 2:1 ratios were determined based on the MICs of cefoperazone (MICs ≤ 8 mg/L denoting susceptibility, 16–32 mg/L indicating intermediate and ≥64 mg/L denoting resistance) [30]. *Escherichia coli* ATCC 25922 was used as the quality control strain.

4.3. Conjugation and Chemical Transformation Experiments

To determine the transferable ability of the Hgz_103-type plasmid carrying *bla*_{OXA-23} in the *A. baumannii* ZHOU strain, conjugation experiments using a rifampicin-resistant derivative of *A. baumannii* ATCC 17978 as the recipient strain were performed using the film mating method [1,18]. Transconjugants were selected on MH agar plates containing rifampicin (50 mg/L) and imipenem (2 mg/L). Donor or recipient bacteria culture alone was used as the control. The identity of transconjugants was confirmed via PCR. Experiments were carried out in triplicate independently.

Chemical transformation assays were further performed when conjugation experiments failed. The plasmid-harboring *bla*_{OXA-23} gene was transferred into *E. coli* DH5α via chemical transformation with imipenem (2 mg/L) for selection [31].

4.4. Whole-Genome Sequencing (WGS) and Phylogenetic Analysis

Genomic DNA was extracted from *A. baumannii* DETAB-C9, DETAB-P65 and ZHOU using a Qiagen minikit (Qiagen, Hilden, Germany) in accordance with the manufacturer's instructions, followed by WGS with the Illumina HiSeq platform (Illumina, San Diego, CA, USA) and the MinION (Nanopore, Oxford, UK) platform (Weishu, Zhejiang, China). De novo assembly of the short and long reads was constructed using Unicycler v0.4.8 [32].

Assembly sequence quality was checked through QUAST v. 5.0.2 [33]. Genome sequence was annotated using both National Center for Biotechnology Information Prokaryotic Genome Annotation Pipeline (NCBI-PGAP) (http://www.ncbi.nlm.nih.gov/genome/annotation_prok/) (accessed on 7 September 2022) and Prokka 1.14.0 [34]. Pasteur [35] and Oxford [36] MLST schemes were performed via PubMLST (<https://pubmlst.org/>) (accessed on 7 September 2022). For antimicrobial resistance profiles, ABRicate v0.8.13 was utilized with the ResFinder database [37]. Point mutations concerning resistance were identified using the fIDBAC software [38]. Virulence factors were detected via the virulence factor database (VFDB) [39]. Insertion sequences (ISs) and transposons were identified using ISFinder and The Transposon Registry [40,41]. *oriT*finder was used to recognize the origin of transfers (*oriT*) and mobile genetic elements (MGEs) [42]. The capsular polysaccharide (K locus) and lipooligosaccharide (OC locus) were analyzed by Bautype [43] and *Kaptive* [19], respectively. Recombinase recognition sites XerC/XerD (C/D) and XerD/XerC (D/C) were tested using *pdif*Finder (<http://pdif.dmicrobe.cn/pdif/home/>) (accessed on 7 September 2022) [44]. The PHAge Search Tool (PHASTER) was utilized for bacteriophage prediction [45]. Plasmid structure was visualized with Proksee (<https://proksee.ca/projects/new>) (accessed on 7 September 2022). Plasmid comparison with ZW85p2 (accession number: CP006769) was performed using Easyfig [46] and visualized with Adobe Illustrator CC 2021. Phylogenetic analysis of all ST46 *A. baumannii* strains was performed using Snippy v4.4.5 (<https://github.com/tseemann/snippy>) (accessed on 21 September 2022) and FastTree using RAxML under the GTRGAMMA model with DETAB-C9 as the reference strain [47]. Generation tree file was visualized using iTOL v5 (<https://itol.embl.de/>) (accessed on 27 September 2022) [48]. Single nucleotide polymorphisms (SNPs) were calculated using SNP-dists V0.6.3 (<https://github.com/tseemann/snp-dists>) (accessed on 27 September 2022) [49], and the matrix was further visualized with RStudio v3.5.3.

4.5. Pan-Genome Analysis

Pan-genome analysis of all ST46_{Pas} *A. baumannii* strains from NCBI GenBank Assembly database was conducted using the BacWGSTdb server to search the close genetic relationship strains with the parameter of 100 SNPs threshold [50]. In brief, Roary v3.11.2 pipeline [51] was used to perform the pan-genome analysis using the GFF files generated by Prokka, with a blastp percentage identity of 95% and a core definition of 99%. Based on the pan-genome analysis, four various classes of genes were classified, including “core” (99% ≤ strains ≤ 100%), “soft core” (95% ≤ strains < 99%), “shell” (15% ≤ strains < 95%) and “cloud” (0% ≤ strains < 15%) groups, respectively [52]. Gene presence/absence file was further visualized with the tree file using the phandango website (<https://jameshadfield.github.io/phandango>) (accessed on 27 September 2022).

4.6. Nucleotide Sequence Accession Numbers

The complete genome assemblies of the chromosome and plasmids from *A. baumannii* DETAB-C9, DETAB-P65 and ZHOU are available from GenBank under accession numbers CP104295-CP104296, CP077835-CP077836 and CP104297-CP104299, respectively.

5. Conclusions

This study describes, for the first time, the genomic characteristics of ST46_{Pas} OXA-23-producing CRAB isolates. Possible evolutionary pathways indicate that the strains emerged via translocation events of the IS*Aba1*-related Tn7534 composite transposon or the *pdif* module. Thus far, ST46_{Pas} CRAB strains have been mainly recovered from hospitals in Hangzhou, China. Nonetheless, effective surveillance should be implemented for ST46_{Pas} CRAB strains to prevent their dissemination and outbreaks in China and globally.

Supplementary Materials: The following supporting information can be downloaded at: <https://www.mdpi.com/article/10.3390/antibiotics12020396/s1>. Figure S1. Pan-genome analysis of ST46_{Pas} *A. baumannii* strains using Roary. (A) The numbers of genes belonging to core, soft-core, shell and cloud groups are shown as a pie chart. (B) Matrix of presence/absence genes generated by Roary and the phylogenetic tree of 11 ST46_{Pas} *A. baumannii* strains. Figure was created using Phandango. Table S1. Site-specific recombinases XerC/XerD (C/D) and XerD/XerC (D/C) in the chromosome of *A. baumannii* ZHOU isolate.

Author Contributions: Conceptualization, X.H. and Y.Y.; methodology, H.L. and X.L.; validation, H.L. and J.H.; formal analysis, J.H., L.Z. and Z.Z.; investigation, H.L. and F.Z.; data curation, H.L.; writing—original draft preparation, H.L.; writing—review and editing, X.H. and Y.Y.; visualization, X.H. and Y.Y.; supervision, X.H. and Y.Y.; project administration, X.H. and Y.Y.; funding acquisition. All authors have read and agreed to the published version of the manuscript.

Funding: This work was undertaken with the support of the National Key Research and Development Program of China grant (2018YFE0102100) and the National Natural Science Foundation of China (81861138054, 82072313).

Institutional Review Board Statement: The study was conducted in accordance with the Declaration of Helsinki and approved by the local Ethics Committee of Sir Run Run Shaw Hospital (approval number 20190802-1).

Informed Consent Statement: This study was approved by the Sir Run Run Shaw Hospital (SRRSH) local ethics committee, Zhejiang University (approval number 20190802-1) and informed consent was obtained before sampling.

Data Availability Statement: The complete genome assemblies of the chromosome and plasmids from *A. baumannii* DETAB-C9, DETAB-P65 and ZHOU are available from GenBank under accession numbers CP104295–CP104296, CP077835–CP077836 and CP104297–CP104299, respectively. The data link for reviewers is <https://www.ncbi.nlm.nih.gov/search/all/?term=PRJNA738868> (accessed on 17 June 2021) and <https://www.ncbi.nlm.nih.gov/search/all/?term=+PRJNA877402> (accessed on 7 September 2022).

Acknowledgments: We thank Sebastian Leptihn from Germany for the careful modification of this manuscript.

Conflicts of Interest: The funders had no role in the design of the study; in the collection, analyses or interpretation of data; in the writing of the manuscript; or in the decision to publish the results.

References

1. Liu, H.; Moran, R.A.; Chen, Y.; Doughty, E.L.; Hua, X.; Jiang, Y.; Xu, Q.; Zhang, L.; Blair, J.M.A.; McNally, A.; et al. Transferable *Acinetobacter baumannii* plasmid pDETAB2 encodes OXA-58 and NDM-1 and represents a new class of antibiotic resistance plasmids. *J. Antimicrob. Chemother.* **2021**, *76*, 1130–1134. [CrossRef]
2. Hamidian, M.; Nigro, S.J. Emergence, molecular mechanisms and global spread of carbapenem-resistant *Acinetobacter baumannii*. *Microb. Genom.* **2019**, *5*, e000306. [CrossRef]
3. Rando, E.; Segala, F.V.; Vargas, J.; Seguiti, C.; De Pascale, G.; Murri, R.; Fantoni, M. Cefiderocol for Severe Carbapenem-Resistant *A. baumannii* Pneumonia: Towards the Comprehension of Its Place in Therapy. *Antibiotics* **2021**, *11*, 3. [CrossRef]
4. Perez, S.; Innes, G.K.; Walters, M.S.; Mehr, J.; Arias, J.; Greeley, R.; Chew, D. Increase in Hospital-Acquired Carbapenem-Resistant *Acinetobacter baumannii* Infection and Colonization in an Acute Care Hospital During a Surge in COVID-19 Admissions—New Jersey, February–July 2020. *Morb. Mortal. Wkly. Rep.* **2020**, *69*, 1827–1831. [CrossRef]
5. Liepa, R.; Mann, R.; Osman, M.; Hamze, M.; Gunawan, C.; Hamidian, M. Cl415, a carbapenem-resistant *Acinetobacter baumannii* isolate containing four AbaR4 and a new variant of AbGRI2, represents a novel global clone 2 strain. *J. Antimicrob. Chemother.* **2022**, *77*, 345–350. [CrossRef]
6. Kim, D.H.; Choi, J.Y.; Kim, H.W.; Kim, S.H.; Chung, D.R.; Peck, K.R.; Thamlikitkul, V.; So, T.M.; Yasin, R.M.; Hsueh, P.R.; et al. Spread of carbapenem-resistant *Acinetobacter baumannii* global clone 2 in Asia and AbaR-type resistance islands. *Antimicrob. Agents Chemother.* **2013**, *57*, 5239–5246. [CrossRef]
7. Liu, L.L.; Ji, S.J.; Ruan, Z.; Fu, Y.; Fu, Y.Q.; Wang, Y.F.; Yu, Y.S. Dissemination of blaOXA-23 in *Acinetobacter* spp. in China: Main roles of conjugative plasmid pAZJ221 and transposon Tn2009. *Antimicrob. Agents Chemother.* **2015**, *59*, 1998–2005. [CrossRef]
8. Fedrigo, N.H.; Xavier, D.E.; Cerdeira, L.; Fuga, B.; Marini, P.V.B.; Shinohara, D.R.; Carrara-Marroni, F.E.; Lincopan, N.; Tognim, M.C.B. Genomic insights of *Acinetobacter baumannii* ST374 reveal wide and increasing resistome and virulome. *Infect. Genet. Evol.* **2022**, *97*, 105148. [CrossRef]

9. Lee, H.-Y.; Chang, R.-C.; Su, L.-H.; Liu, S.-Y.; Wu, S.-R.; Chuang, C.-H.; Chen, C.-L.; Chiu, C.-H. Wide spread of Tn2006 in an AbaR4-type resistance island among carbapenem-resistant *Acinetobacter baumannii* clinical isolates in Taiwan. *Int. J. Antimicrob. Agents* **2012**, *40*, 163–167. [[CrossRef](#)]
10. Zhao, F.; Liu, H.; Yao, Y.; Zhang, L.; Zhou, Z.; Leptihn, S.; Yu, Y.; Hua, X.; Fu, Y. Description of a Rare Pyomelanin-Producing Carbapenem-Resistant *Acinetobacter baumannii* Strain Coharboring Chromosomal OXA-23 and NDM-1. *Microbiol. Spectr.* **2022**, *10*, e0214422. [[CrossRef](#)]
11. Hua, X.; Xu, Q.; Zhou, Z.; Ji, S.; Yu, Y. Relocation of Tn2009 and characterization of an ABGR13-2 from re-sequenced genome sequence of *Acinetobacter baumannii* MDR-ZJ06. *J. Antimicrob. Chemother.* **2019**, *74*, 1153–1155. [[CrossRef](#)]
12. Wareth, G.; Abdel-Glil, M.Y.; Schmoock, G.; Steinacker, U.; Kaspar, H.; Neubauer, H.; Sprague, L.D. Draft Genome Sequence of an *Acinetobacter baumannii* Isolate Recovered from a Horse with Conjunctivitis in Germany. *Microbiol. Resour. Announc.* **2019**, *8*, e01128-19. [[CrossRef](#)]
13. Zhang, J.; Xie, J.; Li, H.; Wang, Z.; Yin, Y.; Wang, S.; Chen, H.; Wang, Q.; Wang, H. Genomic and Phenotypic Evolution of Tigecycline-Resistant *Acinetobacter baumannii* in Critically Ill Patients. *Microbiol. Spectr.* **2022**, *10*, e0159321. [[CrossRef](#)]
14. Schultz, M.B.; Pham Thanh, D.; Tran Do Hoan, N.; Wick, R.R.; Ingle, D.J.; Hawkey, J.; Edwards, D.J.; Kenyon, J.J.; Phu Huong Lan, N.; Campbell, J.I.; et al. Repeated local emergence of carbapenem-resistant *Acinetobacter baumannii* in a single hospital ward. *Microb. Genom.* **2016**, *2*, e000050. [[CrossRef](#)]
15. Douraghi, M.; Kenyon, J.J.; Aris, P.; Asadian, M.; Ghourchian, S.; Hamidian, M. Accumulation of Antibiotic Resistance Genes in Carbapenem-Resistant *Acinetobacter baumannii* Isolates Belonging to Lineage 2, Global Clone 1, from Outbreaks in 2012–2013 at a Tehran Burns Hospital. *mSphere* **2020**, *5*, e00164-20. [[CrossRef](#)]
16. Liu, W.; Wu, Z.; Mao, C.; Guo, G.; Zeng, Z.; Fei, Y.; Wan, S.; Peng, J.; Wu, J. Antimicrobial Peptide Cec4 Eradicates the Bacteria of Clinical Carbapenem-Resistant *Acinetobacter baumannii* Biofilm. *Front. Microbiol.* **2020**, *11*, 1532. [[CrossRef](#)]
17. Islam, M.M.; Kim, K.; Lee, J.C.; Shin, M. LeuO, a LysR-Type Transcriptional Regulator, Is Involved in Biofilm Formation and Virulence of *Acinetobacter baumannii*. *Front. Cell. Infect. Microbiol.* **2021**, *11*, 738706. [[CrossRef](#)]
18. Moran, R.A.; Liu, H.; Doughty, E.L.; Hua, X.; Cummins, E.A.; Liveikis, T.; McNally, A.; Zhou, Z.; van Schaik, W.; Yu, Y. GR13-type plasmids in *Acinetobacter* potentiate the accumulation and horizontal transfer of diverse accessory genes. *Microb. Genom.* **2022**, *8*, 000840. [[CrossRef](#)]
19. Wyres, K.L.; Cahill, S.M.; Holt, K.E.; Hall, R.M.; Kenyon, J.J. Identification of *Acinetobacter baumannii* loci for capsular polysaccharide (KL) and lipooligosaccharide outer core (OCL) synthesis in genome assemblies using curated reference databases compatible with Kaptive. *Microb. Genom.* **2020**, *6*, e000339. [[CrossRef](#)]
20. Gorbunova, V.; Seluanov, A.; Mita, P.; McKerrow, W.; Fenyő, D.; Boeke, J.D.; Linker, S.B.; Gage, F.H.; Kreiling, J.A.; Petrashen, A.P.; et al. The role of retrotransposable elements in ageing and age-associated diseases. *Nature* **2021**, *596*, 43–53. [[CrossRef](#)]
21. Hua, X.; Liang, Q.; Deng, M.; He, J.; Wang, M.; Hong, W.; Wu, J.; Lu, B.; Leptihn, S.; Yu, Y.; et al. BacAnt: A Combination Annotation Server for Bacterial DNA Sequences to Identify Antibiotic Resistance Genes, Integrons, and Transposable Elements. *Front. Microbiol.* **2021**, *12*, 649969. [[CrossRef](#)] [[PubMed](#)]
22. Harmer, C.J.; Hall, R.M. IS 26 Family Members IS 257 and IS 1216 Also Form Cointegrates by Copy-In and Targeted Conservative Routes. *mSphere* **2020**, *5*, e00811-19. [[CrossRef](#)] [[PubMed](#)]
23. Harmer, C.J.; Hall, R.M. IS 26-Mediated Formation of Transposons Carrying Antibiotic Resistance Genes. *mSphere* **2016**, *1*, e00038-16. [[CrossRef](#)] [[PubMed](#)]
24. Zhu, Y.; Chen, J.; Shen, H.; Chen, Z.; Yang, Q.W.; Zhu, J.; Li, X.; Yang, Q.; Zhao, F.; Ji, J.; et al. Emergence of Ceftazidime- and Avibactam-Resistant *Klebsiella pneumoniae* Carbapenemase-Producing *Pseudomonas aeruginosa* in China. *mSystems* **2021**, *6*, e0078721. [[CrossRef](#)] [[PubMed](#)]
25. Du, P.; Liu, D.; Song, H.; Zhang, P.; Li, R.; Fu, Y.; Liu, X.; Jia, J.; Li, X.; Fanning, S.; et al. Novel IS26-mediated hybrid plasmid harbouring tet(X4) in *Escherichia coli*. *J. Glob. Antimicrob. Resist.* **2020**, *21*, 162–168. [[CrossRef](#)] [[PubMed](#)]
26. Blackwell, G.A.; Hall, R.M. The tet39 Determinant and the msrE-mpH Genes in *Acinetobacter* Plasmids Are Each Part of Discrete Modules Flanked by Inversely Oriented p dif (XerC-XerD) Sites. *Antimicrob. Agents Chemother.* **2017**, *61*, e00780-17. [[CrossRef](#)]
27. D’Andrea, M.M.; Giani, T.; D’Arezzo, S.; Capone, A.; Petrosillo, N.; Visca, P.; Luzzaro, F.; Rossolini, G.M. Characterization of pABVA01, a plasmid encoding the OXA-24 carbapenemase from Italian isolates of *Acinetobacter baumannii*. *Antimicrob. Agents Chemother.* **2009**, *53*, 3528–3533. [[CrossRef](#)]
28. Loh, B.; Chen, J.; Manohar, P.; Yu, Y.; Hua, X.; Leptihn, S. A Biological Inventory of Prophages in *A. baumannii* Genomes Reveal Distinct Distributions in Classes, Length, and Genomic Positions. *Front. Microbiol.* **2020**, *11*, 579802. [[CrossRef](#)]
29. Krahn, T.; Wibberg, D.; Maus, I.; Winkler, A.; Bontron, S.; Sczyrba, A.; Nordmann, P.; Pühler, A.; Poirel, L.; Schlüter, A. Intraspecies Transfer of the Chromosomal *Acinetobacter baumannii* bla NDM-1 Carbapenemase Gene. *Antimicrob. Agents Chemother.* **2016**, *60*, 3032–3040. [[CrossRef](#)]
30. Lai, C.-C.; Chen, C.-C.; Lu, Y.-C.; Chuang, Y.-C.; Tang, H.-J. In vitro activity of cefoperazone and cefoperazone-sulbactam against carbapenem-resistant *Acinetobacter baumannii* and *Pseudomonas aeruginosa*. *Infect. Drug Resist.* **2019**, *12*, 25–29. [[CrossRef](#)]
31. Weng, X.; Shi, Q.; Wang, S.; Shi, Y.; Sun, D.; Yu, Y. The Characterization of OXA-232 Carbapenemase-Producing ST437 *Klebsiella pneumoniae* in China. *Can. J. Infect. Dis. Med. Microbiol.* **2020**, *2020*, 5626503. [[CrossRef](#)] [[PubMed](#)]
32. Wick, R.R.; Judd, L.M.; Gorrie, C.L.; Holt, K.E. Unicycler: Resolving bacterial genome assemblies from short and long sequencing reads. *PLoS Comput. Biol.* **2017**, *13*, e1005595. [[CrossRef](#)] [[PubMed](#)]

33. Gurevich, A.; Saveliev, V.; Vyahhi, N.; Tesler, G. QCAST: Quality assessment tool for genome assemblies. *Bioinformatics* **2013**, *29*, 1072–1075. [[CrossRef](#)] [[PubMed](#)]
34. Seemann, T. Prokka: Rapid prokaryotic genome annotation. *Bioinformatics* **2014**, *30*, 2068–2069. [[CrossRef](#)]
35. Diancourt, L.; Passet, V.; Nemec, A.; Dijkshoorn, L.; Brisse, S. The population structure of *Acinetobacter baumannii*: Expanding multiresistant clones from an ancestral susceptible genetic pool. *PLoS ONE* **2010**, *5*, e10034. [[CrossRef](#)]
36. Bartual, S.G.; Seifert, H.; Hippler, C.; Luzon, M.A.D.; Wisplinghoff, H.; Rodriguez-Valera, F. Development of a multilocus sequence typing scheme for characterization of clinical isolates of *Acinetobacter baumannii*. *J. Clin. Microbiol.* **2005**, *43*, 4382–4390. [[CrossRef](#)]
37. Zankari, E.; Hasman, H.; Cosentino, S.; Vestergaard, M.; Rasmussen, S.; Lund, O.; Aarestrup, F.M.; Larsen, M.V. Identification of acquired antimicrobial resistance genes. *J. Antimicrob. Chemother.* **2012**, *67*, 2640–2644. [[CrossRef](#)]
38. Liang, Q.; Liu, C.; Xu, R.; Song, M.; Zhou, Z.; Li, H.; Dai, W.; Yang, M.; Yu, Y.; Chen, H. fDBAC: A Platform for Fast Bacterial Genome Identification and Typing. *Front. Microbiol.* **2021**, *12*, 723577. [[CrossRef](#)]
39. Liu, B.; Zheng, D.; Zhou, S.; Chen, L.; Yang, J. VFDB 2022: A general classification scheme for bacterial virulence factors. *Nucleic Acids Res.* **2022**, *50*, D912–D917. [[CrossRef](#)]
40. Siguier, P.; Perochon, J.; Lestrade, L.; Mahillon, J.; Chandler, M. ISfinder: The reference centre for bacterial insertion sequences. *Nucleic Acids Res.* **2006**, *34*, D32–D36. [[CrossRef](#)]
41. Tansirichaiya, S.; Rahman, M.A.; Roberts, A.P. The Transposon Registry. *Mob. DNA* **2019**, *10*, 40. [[CrossRef](#)] [[PubMed](#)]
42. Li, X.; Xie, Y.; Liu, M.; Tai, C.; Sun, J.; Deng, Z.; Ou, H.-Y. oriTfinder: A web-based tool for the identification of origin of transfers in DNA sequences of bacterial mobile genetic elements. *Nucleic Acids Res.* **2018**, *46*, W229–W234. [[CrossRef](#)] [[PubMed](#)]
43. Hua, X.; Liang, Q.; Fang, L.; He, J.; Wang, M.; Hong, W.; Leptihn, S.; Wang, H.; Yu, Y.; Chen, H. Bautype: Capsule and Lipopolysaccharide Serotype Prediction for *Acinetobacter baumannii* Genome. *Infectious Microbes & Diseases.* **2020**, *2*, 18–25. [[CrossRef](#)]
44. Shao, M.; Ying, N.; Liang, Q.; Ma, N.; Leptihn, S.; Yu, Y.; Chen, H.; Liu, C.; Hua, X. Pdif-mediated antibiotic resistance genes transfer in bacteria identified by pdifFinder. *Brief Bioinform* **2023**, *24*, 1–12. [[CrossRef](#)] [[PubMed](#)]
45. Zhou, Y.; Liang, Y.; Lynch, K.H.; Dennis, J.J.; Wishart, D.S. PHAST: A fast phage search tool. *Nucleic Acids Res.* **2011**, *39*, W347–W352. [[CrossRef](#)] [[PubMed](#)]
46. Sullivan, M.J.; Petty, N.K.; Beatson, S.A. Easyfig: A genome comparison visualizer. *Bioinformatics* **2011**, *27*, 1009–1010. [[CrossRef](#)]
47. Lemoine, F.; Correia, D.; Lefort, V.; Doppelt-Azeroual, O.; Mareuil, F.; Cohen-Boulakia, S.; Gascuel, O. NGPhylogeny.fr: New generation phylogenetic services for non-specialists. *Nucleic Acids Res.* **2019**, *47*, W260–W265. [[CrossRef](#)]
48. Letunic, I.; Bork, P. Interactive Tree Of Life (iTOL) v5: An online tool for phylogenetic tree display and annotation. *Nucleic Acids Res.* **2021**, *49*, W293–W296. [[CrossRef](#)]
49. Bush, S.J. Generalizable characteristics of false-positive bacterial variant calls. *Microb. Genom.* **2021**, *7*, 000615. [[CrossRef](#)]
50. Feng, Y.; Zou, S.M.; Chen, H.F.; Yu, Y.S.; Ruan, Z. BacWGSTdb 2.0: A one-stop repository for bacterial whole-genome sequence typing and source tracking. *Nucleic Acids Res.* **2021**, *49*, D644–D650. [[CrossRef](#)]
51. Page, A.J.; Cummins, C.A.; Hunt, M.; Wong, V.K.; Reuter, S.; Holden, M.T.G.; Fookes, M.; Falush, D.; Keane, J.A.; Parkhill, J. Roary: Rapid large-scale prokaryote pan genome analysis. *Bioinformatics* **2015**, *31*, 3691–3693. [[CrossRef](#)] [[PubMed](#)]
52. Carpi, F.M.; Coman, M.M.; Silvi, S.; Picciolini, M.; Verdenelli, M.C.; Napolioni, V. Comprehensive pan-genome analysis of *Lactiplantibacillus plantarum* complete genomes. *J. Appl. Microbiol.* **2022**, *132*, 592–604. [[CrossRef](#)] [[PubMed](#)]

Disclaimer/Publisher’s Note: The statements, opinions and data contained in all publications are solely those of the individual author(s) and contributor(s) and not of MDPI and/or the editor(s). MDPI and/or the editor(s) disclaim responsibility for any injury to people or property resulting from any ideas, methods, instructions or products referred to in the content.